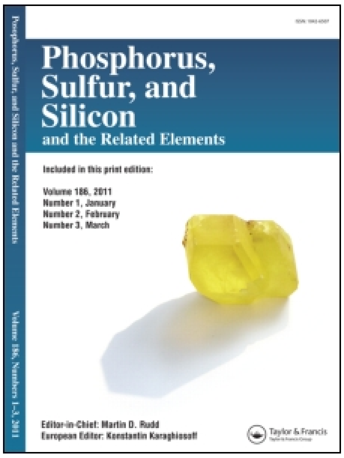

Phosphorus, Sulfur, and Silicon and the Related Elements
Publication details, including instructions for authors and subscription information:
http://www.informaworld.com/smpp/title~content=t713618290

Sulfur-Containing Schiff Base Complexes of Iron(III) and Lead(II): Synthesis, Characterization, Antimicrobial Activity, and Their Electrochemical Behaviors

Sachin Malik[a]; Mamta Kumari[a]; Shikha Chauhan[a]; D. K. Sharma[a]
[a] Department of Chemistry, University of Rajasthan, Jaipur, India

To cite this Article Malik, Sachin , Kumari, Mamta , Chauhan, Shikha and Sharma, D. K.(2010) 'Sulfur-Containing Schiff Base Complexes of Iron(III) and Lead(II): Synthesis, Characterization, Antimicrobial Activity, and Their Electrochemical Behaviors', Phosphorus, Sulfur, and Silicon and the Related Elements, 185: 8, 1759 — 1771

To link to this Article: DOI: 10.1080/10426500903299869

URL: http://dx.doi.org/10.1080/10426500903299869

Phosphorus, Sulfur, and Silicon, 185:1759–1771, 2010

ISSN: 1042-6507 print / 1563-5325 online
DOI: 10.1080/10426500903299869

SULFUR-CONTAINING SCHIFF BASE COMPLEXES OF IRON(III) AND LEAD(II): SYNTHESIS, CHARACTERIZATION, ANTIMICROBIAL ACTIVITY, AND THEIR ELECTROCHEMICAL BEHAVIORS

Sachin Malik, Mamta Kumari, Shikha Chauhan, and D. K. Sharma
Department of Chemistry, University of Rajasthan, Jaipur, India

The sulfur–nitrogen donor ligands, thiosemicarbazones of 5-nitro-1H-indole-2,3-dione and 6-nitro-1H-indole-2,3-dione and 5-chloro-1H-indole-2,3-dione, have been prepared by the condensation of thiosemicarbazide with respective ketones in 1:1 molar ratio in ethanol medium. Lead and iron complexes were prepared by the reaction of lead(II) chloride and iron(III) chloride with the ligands in a 1:2 molar ratio, respectively. The newly synthesized complexes have been characterized by elemental analysis, melting point determinations, and UV, ESR, and IR spectral studies. In all the complexes, the monobasic bidentate nature of the ligand is evident. Based on analytical and spectral data, hexacoordinated structure for lead and pentacoordinated structure for iron complexes have been proposed. Antibacterial and antifungal studies of these compounds against various pathogenic bacterial and fungal strains have been carried out. One of the ligands and its metal complexes were screened for their antifertility activity.

Supplemental materials are available for this article. Go to the publisher's online edition of **Phosphorus, Sulfur, and Silicon and the Related Elements** ***to view the free supplemental file.***

Keywords Antifertility activity; 5-chloro-1H-indole-2,3-dione; 5-nitro-1H-indole-2,3-dione; 6-nitro-1H-indole-2,3-dione; Pb(II) complexes

INTRODUCTION

Compounds with the structure of $-C{=}N-$ (azomethine group) are known as Schiff bases, which are usually synthesized from the condensation of primary amines and active carbonyl groups. Schiff bases are an important class of compounds in the medicinal and pharmaceutical fields.

Schiff base complexes have remained an important and popular area of research due to their simple synthesis, versatility, and diverse range of applications.[1,2] In the area of bioinorganic chemistry, interest in Schiff base complexes with transition and inner-transition metals

---

Received 20 March 2009; accepted 31 August 2009.

One of the authors is thankful to the coordinator of CAS (Centre of Advanced Studies) UGC for JRF, and Head, Department of Chemistry, University of Rajasthan, Jaipur, for providing laboratory facilities.

Address correspondence to D. K. Sharma, Department of Chemistry, University of Rajasthan, Jaipur 302004, India. E-mail: sharma-dk@uniraj.ernet.in

has centered on the role of such complexes in providing synthetic interesting models for the metal-containing sites in metallo-proteins and -enzymes,[3–9] whereas, unsymmetrical Schiff base ligands have clearly offered many advantages over their symmetrical counterparts in the elucidation of the composition and geometry of the metal ion binding sites in the metallo-proteins and -enzymes and selectivity of natural systems with synthetic materials.[10] Furthermore, recent years have witnessed a great deal of interest in the synthesis and characterization of transition metal complexes containing Schiff bases as ligands due to their applications as catalysts for many reactions[11] and their relation to synthetic and natural oxygen carriers.[12] They show biological applications including antimicrobial,[13] antifertility,[14] and antitumor activities.[15] The well-documented biological activities of several N-heterocyclic thiosemicarbazones have often been attributed to a chelation phenomenon with trace metal ions.

Iron is a crucial component of a variety of metabolic pathway that are involved in DNA synthesis and production of energy. Fe(III) complexes of imines have also been found to exhibit biological activity against bacteria.[16] Lead has been used in electric storage batteries, paint pigments, gasoline additives, pipes, ammunition, and solder for many years due to its abundance and physical properties, which also makes it one of the most significant pollutants.[17,18] In addition, since it is slowly eliminated, lead accumulates in liver, kidneys, bones, and other parts of the body.[19] So, the design of drugs to counteract the effects of lead poisoning requires establishing the preferred ligands of Pb(II) and their stereochemistry.

In this article, we report the complexes that were synthesized by the reaction of metal [M = Fe (III) or Pb(II)] with monofunctional bidentate ligands.

RESULTS AND DISCUSSION

The bimolar reactions of iron and lead chloride with the monofunctional bidentate N$^\cap$S donor ligands, 5-nitro-3-(indolin-2-one) thiosemicarbazone (L_1H), 6-nitro-3-(indolin-2-one) thiosemicarbazone (L_2H) and 5-chloro-3-(indolin-2-one) thiosemicarbazone (L_3H) can be represented by the following equations:

For iron(III) complexes:

$$FeCl_3 + 2N^\cap SH \xrightarrow[1:2]{M_eOH} [Fe(N^\cap S)_2Cl] + 2\,HCl$$

(Where, N$^\cap$S is the donor system of the ligand)
For lead(II) complexes:

$$PbCl_2 + 2N^\cap SH \xrightarrow[1:2]{M_eOH} PbCl_2(N^\cap SH)_2$$

(Where, N$^\cap$SH is the donor system of the ligand)

All the reactions proceed easily and lead to the formation of the colored solids. The resulting complexes are insoluble in common organic solvents but soluble in methanol, DMSO, THF, and DMF.

The molecular weights of these complexes were determined by the Rast camphor method, which indicates their monomeric nature. The non-electrolytic behavior of these complexes in anhydrous DMF is indicated by the conductance values; for iron complexes the value is 12–21 Ω^{-1} cm^2 mol^{-1} and lead complexes have low conductance values of 10–15 Ω^{-1} cm^2 mol^{-1}.

Table I IR spectral data (cm^{-1}) of the ligands and their iron(III) complexes

Compound	ν(C=N)	$\nu(NH_2)$	ν(Fe-N)	ν(Fe-S)	ν(Fe-Cl)
L_3H	1620	3500–3338	—	—	—
L_1H	1618	3430–3345	—	—	—
L_2H	1610	3445–3320	—	—	—
$FeCl(L_3)_2$	1615	3440–3335	438	299	357
$FeCl(L_1)_2$	1603	3448–3318	442	306	363
$FeCl(L_2)_2$	1596	3442–3323	440	300	360

Spectroscopy

Electronic spectra. The electronic spectra of the ligands and their complexes were recorded in dry methanol. The electronic spectra of the ligands L_1H, L_2H, and L_3H exhibit broad maxima in the range 350–345 nm due to the n–π^* electronic transitions of the azomethine group, which undergoes a bathochromic shift in the lead and iron complexes, due to the polarization within the >C=N chromophore caused by the metal–ligand interactions. The electronic spectra of the ligands show two maxima at ~272 and ~318 nm assigned to π–π^* electronic transitions within the benzene ring of the ligands. These bands remain almost unchanged in the corresponding metal complexes. The shift is due to the metal–ligand electronic interaction during the chelation.[20]

IR spectra. Upon comparing the IR spectra of the ligands to that of the corresponding lead and iron complexes, it can be concluded that the complex formation takes place through the bonding of nitrogen and sulfur of the ligand moieties. The IR spectra of the ligands (Table I) display sharp bands around 3500–3320 cm^{-1} assignable to NH_2 group.[21] These bands remain unchanged in the complexes, indicating their non-involvement in coordination. Two medium-intensity bands in the regions 3240–3230 cm^{-1} and 1050–1040 cm^{-1} due to ν(NH) and ν(C=S) vibrations, respectively, in the ligands disappear in the spectra of the complexes, which indicates that complexation takes place through the nitrogen and sulfur atoms. In the ligands, the most significant band in the region 1620–1610 cm^{-1} assignable to the ν(C=N) group[22] shifts to the lower frequency in the complexes suggesting the coordination[23,24] of the azomethine nitrogen to the metal atom. A band due to ν(Pb-Cl) at 345–330 cm^{-1} is observed in the lead complexes. The presence of ν(Fe-Cl) vibrations at 363–357cm^{-1} is also observed in the case of iron complexes. The coordination of the azomethine nitrogen and bonding of the thiolic sulfur to the metal ion is also supported by the appearance of nonligand bands in the regions 442–438, 306–299, and 440–425 cm^{-1} in the complexes, which may be assigned to $\nu(Fe\leftarrow N)$, ν(Fe-S), and $\nu(Pb\leftarrow N)$[25] vibrations, respectively (Table I).

Magnetic moment of iron(III) complexes. The effective magnetic moment of iron complexes varies between 1.72–1.81 B.M. The value of intermediate spin–state is S = 3/2 ($^4A_2$), showing five-coordinate geometry. This fact has been established for a series of five-coordinate iron(III) thiosemicarbazones[26] and other complexes.[27,28] The electronic spectra of the iron(III) complexes are also in close agreement with those of previously reported iron(III) complexes showing five-coordinate square pyramidal configuration.[29] The small deviation of the anisotropic g-values from 2.0 suggests the electronic configuration of the ground state is $(d_{xz})^2$ $(d_{yz})^2$ $(d_{xy})^1$, showing pentacoordinated geometry.[30,31]

On the basis of the above discussions, the iron(III) complexes show five-coordinated geometry, and the structures in Figure 1 have been proposed.

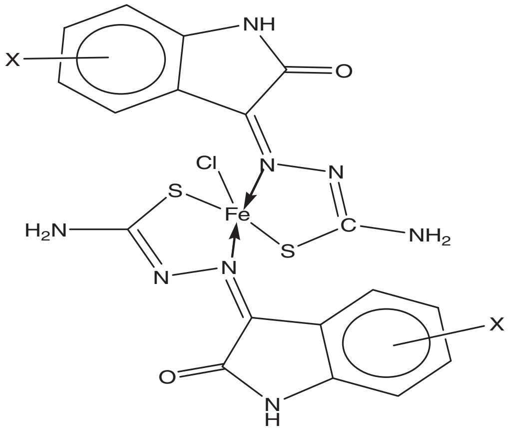

Where, X= 5-NO_2 (L_1H), 6-NO_2 (L_2H), and 5-Cl (L_3H)

Figure 1 Proposed structures of Fe(III) complexes.

NMR spectra of lead(II) complexes. The bonding pattern discussed above gets further support from the ^1H NMR spectra of the ligands and their lead(II) complexes. The ^1H NMR spectra of the free ligands and their metal complexes were recorded in DMSO-d_6. The spectra of the L_1H and L_3H exibit a broad signal at 11.28 and 11.30 due to the NH proton, which disappears in the spectra of lead complexes (Table II). The absence of this signal suggests that this proton has been lost via thioenolization of the C=S group, and coordination of sulfur to the metal ion, has taken place. The multiplets in the region 6.73–8.05 ppm due to aromatic protons, a singlet in the region 3.45–3.48 ppm due to NH_2 group and in the region 11.85–11.88ppm due to NH proton of the ring in the free ligands do not alter in the metal complexes, indicating the noninvolvement of these groups in coordination.[32]

^{13}C NMR spectra of the lead(II) complexes. The ^{13}C NMR spectra of the lead(II) complexes showed a considerable shift of the signals due to (>C=S) and (>C=N) towards the lower field as compared to the ligands.[33] This indicates the coordination of the thiolic sulfur and azomethine nitrogen with the lead atom.

^{13}C NMR spectra of the L_1H and L_3H ligands exhibit signals at 165–166.5 ppm and 155–158.7 ppm due to >C=S and >C=N bonds, respectively. These signals for the lead(II) complexes shifted toward the lower field 158–161 ppm and 148–152 ppm respectively, as compared to the ligand.

Table II ^1H NMR spectral data (δ ppm) of the ligands and their lead(II) complexes

Compound	-NH (ring)	-NH (free)	-NH_2 (s)	Aromatic protons (m)
L_3H	11.85	11.30	3.42	6.89–8.20
L_1H	11.88	11.28	2.80	6.75–8.32
$PbCl_2(L_3H)_2$	11.79	11.25	3.39	7.00–8.01
$PbCl_2(L_1H)_2$	11.76	11.22	2.78	6.88–8.10

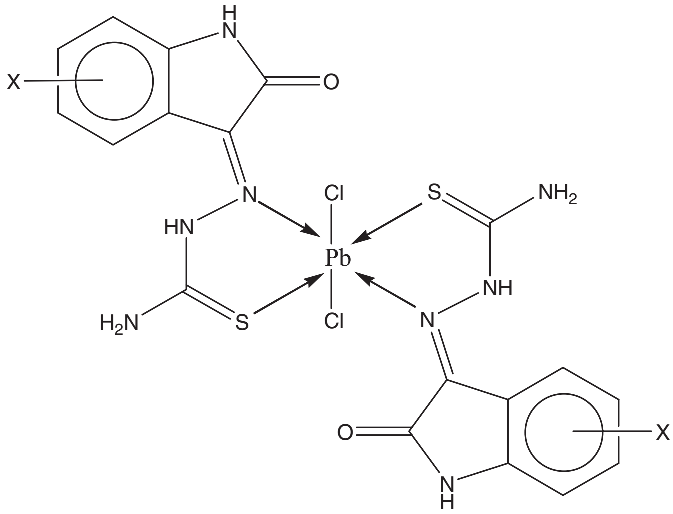

Where, X= 5-NO_2 (L_1H), 6-NO_2 (L_2H), and 5-Cl (L_3H)

Figure 2 Proposed structures of Pb(III) complexes.

On the basis of the above discussion, the geometry shown in Figure 2 can be proposed for the resulting hexa-coordinated complexes. The structures of the ligands are shown in Figure 3.

Antimicrobial Studies

The results of antimicrobial activity (Table S1, Supplemental Materials available online) reveal that the metal complexes showed more antimicrobial activity than do the parent ligands. The increased potency of the metal complexes to the free ligands may be ascribed to the chelation.[34] The chelation increases the lipophilic nature of the central metal atom, which subsequently favors permeation through the lipid layer of the cell membrane. Complexes inhibit the growth of the fungi and bacteria to a greater extent as the concentration is increased.

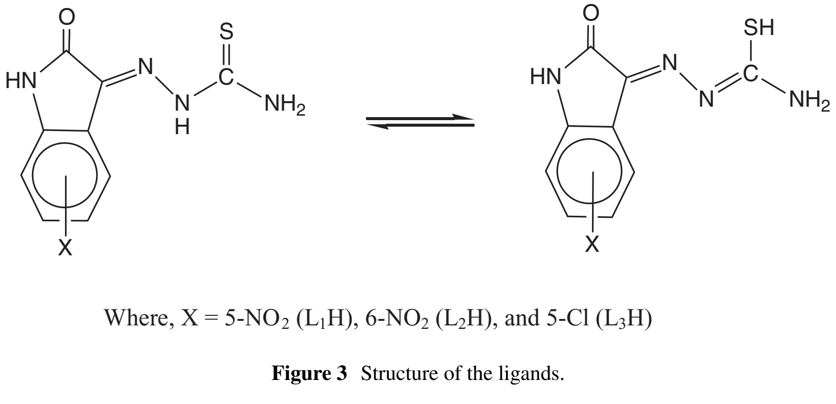

Where, X = 5-NO_2 (L_1H), 6-NO_2 (L_2H), and 5-Cl (L_3H)

Figure 3 Structure of the ligands.

Antifertility Activity

The results reported in Table S2 reveal that there is significant decrease in the motility from 78 ± 5.0 to 37 ± 1.9 in animals treated with the complexes. The sperm density also decreased significantly ($p < 0.001$) from 3.9 ± 0.7 to 2.3 ± 0.5 in testes and from 59 ± 5 to 49 ± 3 in cauda epididymis. The fertility test fluctuates between 65% to 95% negative. Thus the present study reveals that lead complexes are a more effective inhibitor then their respective ligands in male rats.

Electrochemical Study Fe(III) Complex Compound: Voltammetric Behavior

The electrochemical behavior of the Fe(III) complex was studied by cyclic voltammetric techniques on HMDE. In this case, the compound showed two well-defined reduction peaks at −0.45 V and −1.05 V in the nonaqueous solution, which is attributed to the reduction of Fe(III) at HMDE. No peak could be observed in the anodic direction of the reverse scans, suggesting the irreversible nature of the electrode process. The peak potential shifted towards more negative values (Figure 4) with an increase in scan rate, confirming the irreversible nature of the reduction process when the effect of scan rate ($\upsilon^{1/2}$) on stripping peak current (i_p) was examined under the above experimental conditions(Figures 5a and 5b). It was observed that the sweep rate is increased from 50, 100, 200, 400, and 500 mV/s at a fixed concentration (3×10^{-3} M) of the Fe(III) complex. Further it was

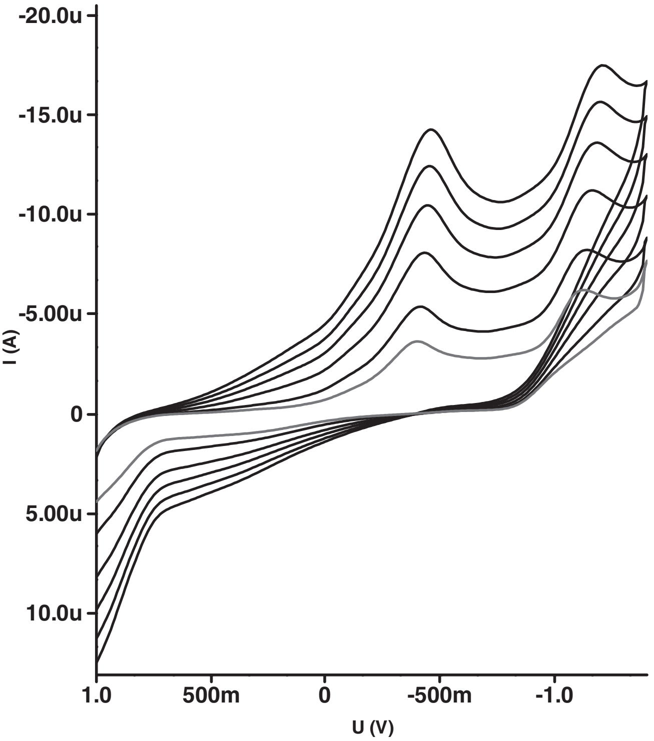

Figure 4 Cyclic voltammogram of Fe(III) complex at different scan rates.

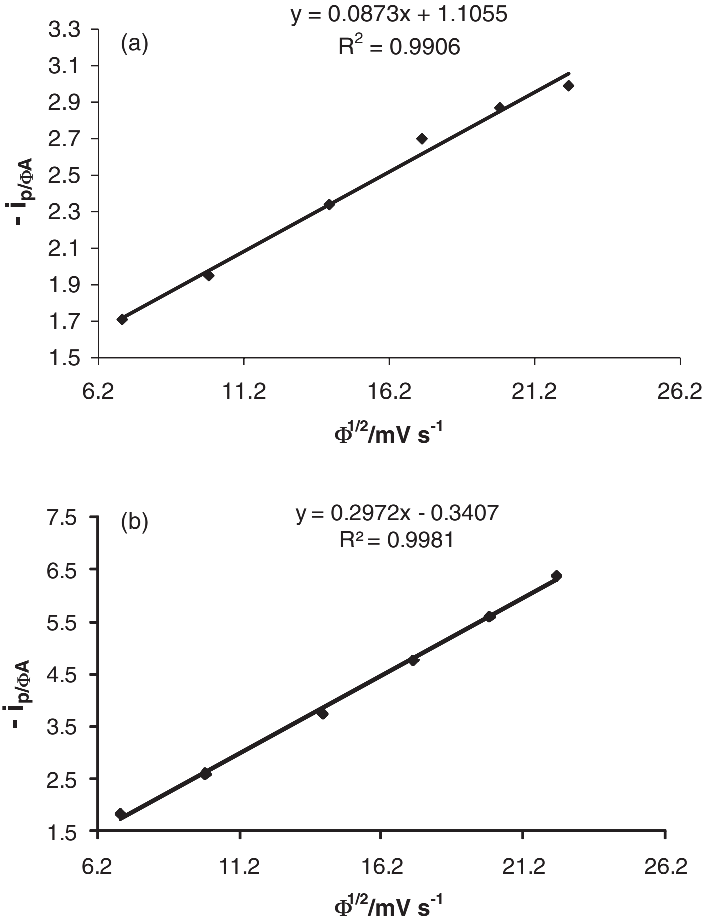

Figure 5 Plot between peak current and square of scan rate for (a) I reduction peak and (b) II reductions peak of Fe(III) complex.

observed that the peak potential shifted cathodically, and the peak current increased steadily. A straight line is obtained when i_p is plotted against $\upsilon^{1/2}$, which may be expressed by the following equation:

For Ist reduction peak

$$y(i_p) = 0.2979\upsilon^{1/2}\ (mV/s) - 0.3407\ (\mu A), r^2 = 0.9981$$

For II reduction

$$y(i_p) = 0.0873\upsilon^{1/2}\ (mV/s) + 1.1055\ (\mu A), r^2 = 0.9906$$

The results also explained the diffusion-controlled nature of the electrode process.

Electrochemical Study of Pb(II) Complex Compound: Voltammetric Behavior

For the study of the electrochemical behavior of the Pb(II) complex, stock solution of (1×10^{-3} M) concentration was used. The diagram in this case gave two well-defined reduction peaks at −0.27 V and −0.90 V in the nonaqueous solution, which is attributed to the reduction of Pb(II) at HMDE. Absence of any peak in the anodic direction of the reverse scans is an indication of the irreversible nature of the electrode process. However, the peak potential shifted towards more negative values (Figure 6) with increase in scan rate, confirming the irreversible nature of the reduction process.

The effect of scan rate ($\upsilon^{1/2}$) on stripping peak current (i_p) was examined under the above experimental conditions (Figures 7a and 7b). As the sweep rate is increased from 50, 100, 200, 400, and 500 mV/s at a fixed concentration (3×10^{-3} M) of Pb(II) complex: (i) the peak potential shifted cathodically, and (ii) the peak current increased steadily. A straight line is obtained when i_p is plotted against $\upsilon^{1/2}$, which may be expressed by the following equation:

For Ist reduction peak

$$y(i_p) = 0.5333\upsilon^{1/2}\ (\text{mV/s}) - 1.1723\ (\mu\text{A}),\ r^2 = 0.9905$$

For II reduction peak

$$y(i_p) = 0.446\upsilon^{1/2}\ (\text{mV/s}) + 0.2795\ (\mu\text{A}),\ r^2 = 0.9865$$

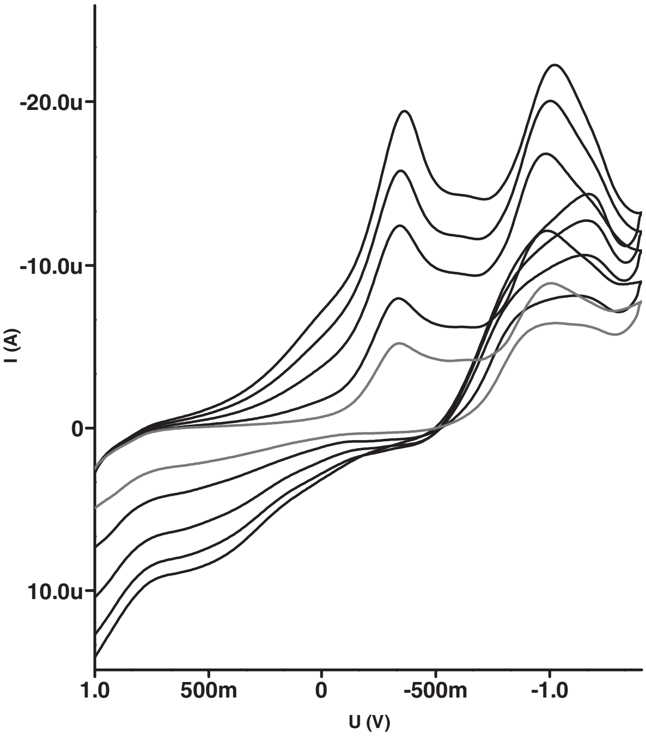

Figure 6 Cyclic voltammogram of Pb(II) complex at different scan rates.

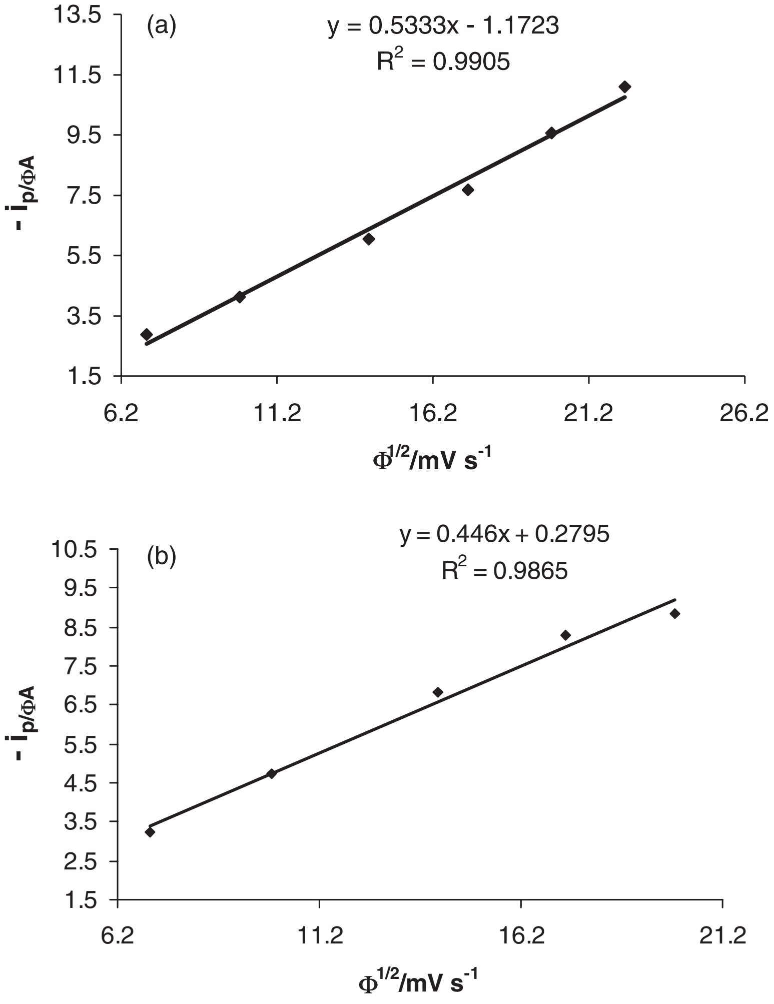

Figure 7 Plot between peak current and square of scan rate for (a) I reduction peak and (b) II reduction peaks of Pb(II)complex.

All these facts pointed towards the diffusion-controlled nature of the electrode process.

CONCLUSION

Based on various physicochemical and structural investigations, it was concluded that the ligands act as bidentate ligands forming pentacoordinated with Fe(III) and hexacoordinated with Pb(II). Furthermore, the current study strongly demonstrates that the iron and lead complexes are more effective antimicrobial and antifertility agents than the parent ligands. Voltammetric behavior of Fe(III) and Pb(II) complexes clearly indicates the diffusion-controlled nature of the electrode process.

EXPERIMENTAL

Physical Measurements and Analytical Methods

Molecular weights of the newly synthesized ligands and their metal complexes were determined by the Rast camphor method. Sulfur and nitrogen were estimated by Messenger's and Kjeldahl's methods, respectively. Copper was estimated volumetrically. ESR spectra of the complexes were monitored on Varian E-4X band spectrometer. The electronic spectra were recorded on a Varian–Cary/5E spectrophotometer at SAIF, IIT, Madras, Chennai. Infrared spectra of the ligands and their complexes were recorded in the region 4000–200 cm^{-1} with the help of a Nicolet Megna FTIR-550 spectrophotometer on KBr pellets. Voltammetric measurements were performed with a Metrohm Computrace Voltammetric Analyzer μ AUTOLAB Type III Potentiostat Ecochemie (Utrecht, The Netherlands) Model 757 VA. A conventional three-electrode system was used, which consisted of an Ag/AgCl/KCl reference electrode, a hanging mercury drop electrode (HMDE) as a working electrode, and a graphite rod as an auxillary electrode. The whole measurements were automated and controlled through the programming capacity of the apparatus. The data were treated through a PC connected to the Electrochemical Analyzer Version-757 VA Computrace.

Synthesis of Thio-Schiff Bases

5-Nitro-1H-indole-2,3-dione, 6-nitro-1H-indole-2,3-dione,[35] and 5-chloro-1H-indole-2,3-dione[36] were prepared by methods reported earlier. The ligands, thiosemicarbazones of 5-nitro-1H-indole-2,3-dione, 6-nitro-1H-indole-2,3-dione and 5-chloro-1H-indole-2,3-dione, were prepared by the condensation of thiosemicarbazide with respective ketones in 1:1 molar ratio in ethanol by the condensation method.[37] Their physicochemical properties and analytical data are given in Table III. The parent ligands exist in the tautomeric forms (Figure 3).

Table III Analytical data and physical properties of the ligands and their iron and lead complexes

Compound	Molar ratio	Color	Melting point (°C)	Found (calcd.) (%) N	S	M	Mol. wt. found (calcd.)
$C_9H_7N_5O_3S$	—	Dark brown	247	26.32	12.26	—	249.54
(L^1H)				(26.40)	(12.08)		(265.24)
$C_9H_7N_5O_3S$	—	Gray	221	26.16	12.24	—	281.42
(L^2H)				(26.40)	(12.08)		(265.41)
$C_9H_7N_4OSCl$	—	Dim yellow	257	22.12	12.54	—	270.17
(L^3H)				(21.99)	(12.58)		(254.69)
$FeCl(L_1)_2$	1:2	Dark brown	100–105	(22.59)	(10.34)	(9.01)	(619.76)
				22.68	10.27	8.91	634.11
$FeCl(L_2)_2$	1:2	Dark green	148–152	(22.59)	(10.34)	(9.01)	(619.76)
				22.68	10.27	8.91	634.11
$FeCl(L_3)_2$	1:2	Dark brown	175–180	(18.71)	(10.71)	(9.32)	(598.09)
				18.79	10.65	9.25	584.18
$PbCl_2(L_1H)_2$	1:2	Yellow	100–105	17.18	8.11	25.67	794.95
				(17.29)	(8.07)	(25.58)	(809.73)
$PbCl_2(L_3H)_2$	1:2	Yellow	175–180	41.12	6.35	26.35	773.89
				(41.21)	(6.28)	(26.27)	(788.69)

Synthesis of the Complexes

Iron(III)chloride (4.99 mmol) was reacted with the ligands [L_1H (10.45 mmol), L_2H (9.27 mmol), and L_3H (9.29 mmol)] in bimolar ratio in dry methanol (40 mL). This resulted in the liberation of HCl. The reaction mixture was thoroughly shaken and then refluxed for 5 to 7 h on a fractionating column. The excess solvent was distilled off after the completion of the reaction, and the compound was repeatedly washed with *n*-hexane and then dried in vacuo for 1 h to yield the final purified product. Lead(II) chloride (3.23 mmol) was reacted with the ligands [L_1H (6.85 mmol), L_2H (6.02 mmol), and L_3H (6.02 mmol)] in bimolar ratio in dry methanol. This reaction must be allowed to occur with rapid stirring as well as refluxing for a sufficiently long time, usually 2 to 5 days, to ensure completion as determined by the constant composition of the product. Lead chloride probably dissolves slightly under these conditions to form adducts of such low solubility that they precipitate.

The synthetic data, physical properties, and analytical data of the compounds are listed in Table III.

Antifungal Activity

Potato dextrose agar medium was prepared in flask and sterilized. The percentage inhibition of growth was calculated by (C—T) $C^{-1} \times 100$, where C and T are the diameter of the fungus colony in the control and test plates, respectively.[38] See the Supplemental Materials, Tables S1 and S 2, for Experimental details and results (available online).

Antibacterial Activity

Flat-bottomed Petri discs were used, and nearly 15 mL of the beef extract medium (peptone 5g, beef extract 5g, NaCl 5g, and agar 20 g) and distilled water (1000 mL) were pipetted out into the Petri disc. These Petri discs were incubated for 24 h at 25 ± 2 °C, and the zone of inhibition[39] was measured in mm.

Antifertility Activity

Healthy Sprague Dawley albino rats (*Rattus novegicus*) weighing 170–200 g were chosen for experimentation.

Electrochemical Study

Stock solution of 1×10^{-3} M was prepared in dimethyl formamide (DMF). 1 M tetraethyl ammonium perchlorate (TEAP) in DMF was used as supporting electrolyte. All reagents and solvents were of analytical grade (Merck and Sigma).

Voltammetric measurements were performed with a Metrohm Computrace Voltammetric Analyzer μ AUTOLAB Type III Potentiostat Ecochemie (Utrecht, The Netherlands) Model 757 VA. A conventional three-electrode system was used that consisted of an Ag/AgCl/KCl reference electrode, a hanging mercury drop electrode (HMDE) as a working electrode, and a graphite rod as an auxillary electrode.[40,41] The whole measurements were automated and controlled through the programming capacity of the apparatus. The data were treated through a PC connected to the Electrochemical Analyzer version-757 VA Computrace.

REFERENCES

1. M. K. Taylor, J. Reglinski, and D. Wallace, *Polyhedron*, **23,** 3201 (2004).
2. S. Yamada, *Coord. Chem. Rev.*, **192,** 537 (1999).
3. A. A. Khandar, S. A. Hosseini-Yazdi, and S.A. Zarei, *Inorg. Chim. Acta*, **358,** 3211 (2005).
4. P. K. Mascharak, *Coord. Chem. Rev.*, **225,** 201 (2002).
5. J. G. Muller, L. A. Kayser, S. J. Paikoff, V. Duarte, N. Tang, R. J. Perez, S. E. Rokita, and C. J. Burrows, *Coord. Chem. Rev.*, **761,** 185 (1999).
6. D. P. Kessissoglou, *Coord. Chem. Rev.*, **837,** 185 (1999).
7. V. E. Kaasjager, L. Puglisi, E. Bouwman, W. L. Driessen, and J. Reedijk, *Inorg. Chim. Acta*, **310,** 183 (2000).
8. A. S. Al-Shihri, *Spectrochim. Acta*, **A60,** 1189 (2004).
9. W. Kaim and B. Schwederski, *Bioinorganic Chemistry: Inorganic Elements in the Chemistry of Life* (Wiley, New York, 1996).
10. N. Daneshvar, A. A. Entezami, A. A. Khandar, and L. A. Saghatforoush, *Polyhedron*, **22,** 1437 (2003).
11. Y. P. Cai, C. Y. Su, A. W. Xu, B. S. Kang, Y. X. Tong, H. Q. Liu, and S. Jie, *Polyhedron*, **20,** 657 (2001).
12. G. Henrici-Oleive and S. Olive, *Coordination and Catalysis* (Weinheim Verlag Chemie, New York, 1977); *The Chemistry of the Catalyzed Hydrogenation of Carbon Monoxide* (Springer Verlag, Berlin, Germany, 1984).
13. A. Bansal, N. Fahmi, and R. V. Singh, *Main Group Met. Chem.*, **26,** 335 (2003).
14. N. Fahmi, C. Saxena, and R. V. Singh, *Bull. Chem. Soc. Jpn.*, **69,** 963 (1996).
15. R. Campo, J. J. Criado, E. Garcia, M. R. Hermosa, A. J. Sanchez, J. L. Manzano, E. Monte, E. R. Fernandez, and F. Sanz, *J. Inorg. Biochem.*, **89,** 74 (2002).
16. M. Omar, G. Mohamed, and A. Hindy, *J. Therm. Anal. Calorim.*, **86,** 315, (2006).
17. B. P. Lanphear, *Science*, **281,** 1617 (1998).
18. B. P. Lanphear and K. Roghmann, *J. Environ. Res.*, **74,** 67 (1997).
19. H. Sigel, C. P. Da Costa, and R. B. Martín, *Coord. Chem. Rev.*, **219,** 435 (2001).
20. M. B. Ferrari, F. Bisceglie, G. Pelosi, M. Sassi, P. Tarasconi, M. Cornia, S. Capacchi, R. Albertini, and S. Pinelli, *J. Inorg. Biochem.*, **90,** 113 (2002).
21. S. Belwal, Seema, N. Fahmi, and R. V. Singh, *Indian J. Chem.*, **38A,** 597 (1999).
22. B. Khem, A. K. Sharma, and N. K. Kaushik, *Polyhedron*, **2,** 1177 (1983).
23. S. Chandra and R. Singh, *Indian. J. Chem.*, **34,** 1003 (2004).
24. N. Kanoongo, R. V. Singh, and J. P. Tandon, *Trans. Met. Chem.*, **15,** 145 (1990).
25. R. H. Holm, G. W. Everett, and A. Chakravarthy, *Progr. Inorg. Chem.*, **7,** 161 (1966).
26. S. K. Jain, B. S. Gary, and Y. K. Bhoon, *Transition Met. Chem.*, **11,** 89 (1986).
27. B. J. Kennedy, G. Brain, and K. S. Murray, *Inorg. Chim. Acta*, **81,** 129 (1982).
28. D. Mansury, I. Margenoterm, M. Lange, and P. Gans, *Inorg. Chem.*, **21,** 1427 (1982).
29. V. M. Leovac, L. S. Jovanovic, L. J. Bjelica, and V. I. Cesljevic, *Polyhedron*, **8,** 135 (1989).
30. Y. Nishida, A. Sumita, K. Hayashida, H. Oshima, S. Kida, and Y. Maeda, *J. Coord. Chem.*, **9,** 161 (1979).
31. N. Matsumoto, K. Kimoto, K. Nishida, A. Ohyoshi, and Y. Maeda, *Chem. Lett.*, 479 (1984).
32. A. K. El-Sawaf, D. X. West, F. A. El-Saied, and R. M. El-Bahnasawy, *Transition Met. Chem.*, **23,** 565 (1998).
33. J. M. Aramini, T. Hiraoki, M. Yazawa, T. Yuan, M. Zhang, and H. J. Vogel, *J. Biol. Inorg. Chem.*, **1,** 39 (1996).
34. A. Ozarowski, B. R. McGarvey, C. Peppe, and D. G. Tuck. *J. Am. Chem. Soc.*, **113,** 3288 (1991).
35. R. Garg, M. K. Saini, N. Fahmi, and R. V. Singh, *Indian J. Chem.*, **44A,** 2433 (2005).
36. R. Garg, M. K. Saini, N. Fahmi, and R. V. Singh, *Trans. Met. Chem.*, **31,** 362 (2006).
37. S. Gaur, N. Fahmi, and R. V. Singh, *Phosphorous, Sulfur, and Silicon*, **182,** 853 (2007).

38. M. K. Biyala, K. Sharma, N. Fahmi, and R. V. Singh, *Phosphorous, Sulfur, and Silicon*, **182,** 2955 (2007).
39. N. Fahmi and R. V. Singh, *J. Ind. Chem. Soc.*, **73**(6), 257 (1996).
40. S. Sharma, D. Wadhwa, G. L. Mourya, and D. K. Sharma. *J. Ultra Chem. Phys. Sci.*, **20**(1), 121 (2008).
41. D. K. Sharma, S. Sharma, G. L. Mourya, and M. Kumari. *J. Indian Chem. Soc.*, **86,** 1 (2009).